



Research paper

The thermal charge-transfer reduction of uranyl UO_2^{2+} (VI) to UO_2^+ (V) by various functionalized organic compounds, and evidence for possible spin-spin interactions between UO_2^+ (V) and hydroxymethyl ($\cdot\text{CH}_2\text{OH}$) radical and between UO_2^+ (V) and diphenyl sulfide radical cation ($\text{Ph}_2\text{S}^{\cdot+}$)

Xiaoping Sun^{a,*}, Derrick R.J. Kolling^b, Seth Deskins^a, Ethan Adkins^b^a Department of Natural Sciences and Mathematics, University of Charleston, Charleston, WV 25304, USA^b Department of Chemistry, Marshall University, Huntington, WV 25755, USA

ARTICLE INFO

Keywords:

Uranyl
Alcohol
Charge-transfer
Oxidation-reduction
EPR
UV-vis
Radical

ABSTRACT

The linear uranyl UO_2^{2+} (VI) cation ($D_{\infty h}$ symmetry) exhibited strong and broad absorptions at 350–400 nm in anhydrous methanol and methanol-water mixtures in the UV-Vis spectra. The intensity of the absorptions (represented by absorbance at 375 nm) is directly proportional to molar concentrations of methanol and UO_2^{2+} (VI), respectively. The linear relationships indicate formation of an electron-donor-acceptor (EDA) complex [UO_2^{2+} , CH_3OH]. The absorptions at 350–400 nm originate from the charge-transfer (single-electron transfer) from CH_3OH (electron donor) to UO_2^{2+} (electron acceptor) within the [UO_2^{2+} , CH_3OH] complex. Electron paramagnetic resonance (EPR) studies of various mixtures of UO_2^{2+} - CH_3OH and UO_2^{2+} - CH_3OH - H_2O have shown that the charge-transfer also took place slowly in the dark, resulting in thermal reduction of UO_2^{2+} (VI) to UO_2^+ (V) (singlet, $g = 2.08$) by CH_3OH , and CH_3OH was oxidized to the hydroxymethyl $\cdot\text{CH}_2\text{OH}$ radical (generating an axial signal). The charge-transfer oxidation-reduction reaction is believed to take place via the EDA [UO_2^{2+} , CH_3OH] complex. EPR studies suggested spin-spin coupling between UO_2^+ (V) and $\cdot\text{CH}_2\text{OH}$ in anhydrous methanol, supporting the formation of a [UO_2^+ , $\cdot\text{CH}_2\text{OH}$] ion-radical pair. The EPR studies have also shown that UO_2^{2+} (VI) was reduced to UO_2^+ (V) thermally by other alcohols (ethanol, 2-propanol, and cyclohexanol), and by diphenyl sulfide (Ph_2S), L-ascorbic acid (AA), and 2-methyl-5-(propan-2-yl)phenol (carvacrol, ArOH), respectively. Ph_2S , AA, and ArOH were oxidized to the diphenyl sulfide $\text{Ph}_2\text{S}^{\cdot+}$ radical cation (singlet, $g = 2.00$), ascorbic acid AA \cdot radical (singlet, $g = 2.00$), and carvacrol ArO \cdot radical (singlet, $g = 1.98$), respectively. Both EPR and UV-Vis studies indicate that the reactions followed the ground-state charge-transfer mechanisms similar to that of the UO_2^{2+} /methanol reaction. EPR evidence supported formation of the [UO_2^+ , $\text{Ph}_2\text{S}^{\cdot+}$] ion-radical pair in the charge-transfer reaction of UO_2^{2+} and Ph_2S and spin-spin interactions within the ion-radical pair. The sulfuric-acid-catalyzed isomerization of $\cdot\text{CH}_2\text{OH}$ to $\text{CH}_3\text{O}\cdot$ was found by EPR studies.

1. Introduction

A particularly interesting chemical property of the linear uranyl UO_2^{2+} (VI) ion (D_{∞} symmetry) is that it possesses a high reduction potential and thus, UO_2^{2+} can oxidize many substances [1]. Since uranium (V) (in the form of UO_2^+) is another readily accessible and relatively stable oxidation state of uranium, the oxidation-reduction chemistry of UO_2^{2+} (diamagnetic) often takes place via a single-electron transfer (charge-transfer) process from a reductant to the valence shell of uranium in UO_2^{2+} [2]. This leads to the formation of paramagnetic UO_2^+ (V), another linear ion, and the reductant (diamagnetic)

upon losing an electron transforms into a radical (Eq. (1)).



Photochemical reduction of uranyl UO_2^{2+} (VI) by many reducing agents have been studied. For example, the UO_2^{2+} -doped polyvinyl alcohol (PVA, $-\text{CH}_2-\text{CH}(\text{OH})-\text{CH}_2-$) film was irradiated by γ -ray (dose 4 kGy). Then an electron paramagnetic resonance (EPR) spectrum was recorded on the γ -irradiated UO_2^{2+} -PVA film, exhibiting a strong broad singlet signal ($g = 2.037$) attributable to UO_2^+ and a weak triplet signal ($g = 2.001$, $a_H = 33$ G) attributable to a PVA \cdot radical ($-\text{CH}_2-\text{C}(\text{OH})-\text{CH}_2-$, an α -hydroxyalkyl radical) [3]. Another example

* Corresponding author.

E-mail address: xiaopingsun@ucwv.edu (X. Sun).<https://doi.org/10.1016/j.ica.2018.07.049>

Received 29 March 2018; Received in revised form 27 July 2018; Accepted 28 July 2018

Available online 31 July 2018

0020-1693/© 2018 Elsevier B.V. All rights reserved.

is the UV-irradiation (using a mercury lamp) of a 1:2 adduct of uranyl (VI) nitrate and tributylphosphate (TBP, $(\text{BuO})_3\text{PO}$), $\text{UO}_2(\text{NO}_3)_2 \cdot 2\text{TBP}$, in *n*-dodecane [4]. In many photochemical reactions of UO_2^{2+} with other reducing agents, such as halides (Br^- and I^-), phenols, and alcohols (methanol, ethanol, and 2-propanol), only radicals (the oxidation products) have been observed by EPR and/or electronic absorption spectroscopy from the reaction mixtures, but the expected reduction product UO_2^+ was not identified [5–8]. The reactions were thought to take place via a charge-transfer from the reductant to the excited state of uranyl(VI) (UO_2^{2+})*. It has been proposed that the lack of UO_2^+ was due to the facile disproportionation of the initially formed UO_2^+ to UO_2^{2+} and U^{4+} at certain photochemical conditions [9].

In a previous paper [2], we reported our discovery of thermal charge-transfer reduction of UO_2^{2+} by halides (Br^- and I^-), DMSO (CH_3SOCH_3), and phenol ($\text{C}_6\text{H}_5\text{OH}$) in the dark. Both UO_2^+ and oxidized radicals (e.g. $\text{C}_6\text{H}_5\text{O}^\cdot$) were observed by EPR and/or electronic absorption spectroscopy. Our work represented investigations of thermal charge-transfer reduction of UO_2^{2+} by any reducing agents for the first time.

In the present paper, we extend our studies to the thermal charge-transfer reduction of UO_2^{2+} by other functionalized organic compounds, including alcohols (methanol, ethanol, 2-propanol, and cyclohexanol), 2-methyl-5-(propan-2-yl)phenol (carvacrol, a biologically relevant substance), diphenyl sulfide, and ascorbic acid. This is the first study of the thermal reduction of UO_2^{2+} by these compounds. For each of the reducing agents, both UO_2^+ and an oxidized radical (e.g., hydroxymethyl, $\cdot\text{CH}_2\text{OH}$) have been observed by EPR spectroscopy from the thermal reaction, while only the radical, but not UO_2^+ , was observable in the previously studied photochemical reactions [5–8].

Direct observation of both UO_2^+ and an oxidized radical (e.g. $\cdot\text{CH}_2\text{OH}$) by EPR in our thermal redox reactions is a significant advance. This way, along with UV-Vis spectroscopic studies, we have demonstrated a charge-transfer mechanism for the reactions via an electron-donor-acceptor (EDA) complex between UO_2^{2+} and a reductant in the ground state. Such a ground-state charge-transfer mechanism for UO_2^{2+} was previously unknown. In addition, we have obtained EPR evidence for the spin-spin interactions between UO_2^+ and the hydroxymethyl $\cdot\text{CH}_2\text{OH}$ radical and between UO_2^+ and diphenyl sulfide $\text{Ph}_2\text{S}^{+\cdot}$ radical cation in ion-radical pairs. Such interactions have not been reported before. In the course of our study, we have found thermal as well as photochemical isomerization of α -hydroxyalkyl radical (e.g. $\cdot\text{CH}_2\text{OH}$) to alkoxy radical (e.g. $\text{CH}_3\text{O}^\cdot$). The formations of two different alcohol radicals in reactions of UO_2^{2+} with methanol, ethanol, and 2-propanol have been confirmed in this work by variable power EPR measurements and computer-aided EPR spectra simulations. We now present our new advances in the studies of thermal charge-transfer reduction of UO_2^{2+} .

2. Experimental

The electronic absorption (UV-visible) spectra were recorded throughout this work using a UV-1601 Shimadzu spectrophotometer which is connected to a Dell computer equipped with Shimadzu UV Probe (Ver. 2.60) software. The data were processed using the Shimadzu UV Probe software installed in the Dell computer.

The Bruker EMXplus EPR spectrometer with microwave frequency 9.37 GHz (X-band) was used for the EPR measurement throughout this work. All spectra were recorded in the frozen state via cooling to 80 K with liquid nitrogen, with microwave power of 5 mW, a modulation amplitude of 15 G, and a modulation frequency of 100 kHz. For each spectrum, background subtraction from the solvent and cavity were performed.

For the variable power EPR measurements, the EPR spectra were measured at various powers with other instrumental parameters unchanged. The peak height for a signal was taken as the intensity of the signal.

The simulation of EPR spectra were performed using EasySpin aided by MATLAB (<http://easyspin.org>) [10].

Uranyl(VI) nitrate hexahydrate [$\text{UO}_2(\text{NO}_3)_2 \cdot 6\text{H}_2\text{O}$] and uranyl(VI) acetate dihydrate [$\text{UO}_2(\text{CH}_3\text{COO})_2 \cdot 2\text{H}_2\text{O}$], both obtained from Sigma-Aldrich Chemical Company, were used as the sources of uranyl(VI) ion (UO_2^{2+}) for the reactions conducted in nearly neutral solutions and in acidic solutions, respectively. Deionized water was used throughout this work. Methanol (anhydrous), ethanol (anhydrous), 2-propanol (95%), and cyclohexanol were obtained from Macron Fine Chemicals. Sulfuric acid (98%) and acetone were obtained from Fisher Chemical. Diphenyl sulfide was obtained from Alfa Aesar. L-Ascorbic acid and 2-methyl-5-(propan-2-yl)phenol (carvacrol) were obtained from Sigma-Aldrich.

In the experiment conducted in each medium throughout the work, the $\text{UO}_2(\text{NO}_3)_2 \cdot 6\text{H}_2\text{O}$ or $\text{UO}_2(\text{CH}_3\text{COO})_2 \cdot 2\text{H}_2\text{O}$ solid was dissolved in the corresponding medium with specific composition at ambient conditions. A UV-visible cell (with thickness of 1 cm) was then filled with each of the UO_2^{2+} solutions, and an electronic absorption (UV-Vis) spectrum was recorded. For EPR measurements, a UO_2^{2+} solution with specific composition was made as above mentioned and incubated in the dark (or irradiated by UV-lamp occasionally) at ambient temperature for a specified time. Then the solution was added into a 4-mm quartz tube that was subsequently placed in the cavity of the spectrometer. The EPR spectrum was recorded in the frozen state at 80 K, with background subtraction as mentioned above.

3. Results and discussion

3.1. Thermal charge-transfer reduction of uranyl UO_2^{2+} (VI) to UO_2^+ (V) by methanol (CH_3OH), and evidence for spin-spin interactions between UO_2^+ (V) and hydroxymethyl radical ($\cdot\text{CH}_2\text{OH}$)

The previous investigations have shown that an excited uranyl (VI) (UO_2^{2+})* possesses particularly strong oxidizing capabilities, allowing it to activate and cleave the relatively inert CH bond in methanol [7,9,11]. However, there has been no report on the thermal oxidation of the methanol CH bond by UO_2^{2+} in the ground state prior to the present work. Although methanol is usually considered a relatively inert solvent towards oxidation-reduction reactions of common oxidants in normal ambient conditions, a thermal redox reaction between UO_2^{2+} and CH_3OH has been identified at normal room temperature in this work. The UO_2^{2+} (as the nitrate salt) solutions in anhydrous CH_3OH and in $\text{CH}_3\text{OH}-\text{H}_2\text{O}$ mixtures were incubated in the dark at ambient temperatures for 24 h and then subjected to EPR spectroscopy in the frozen state at 80 K (Fig. 1). All the spectra showed a broad UO_2^+ signal ($g = 2.08$) and axial and rhombic signals [12]. By referencing to previous EPR studies of methanol radicals in frozen solution [13], the axial signal is attributable to the hydroxymethyl $\cdot\text{CH}_2\text{OH}$ radical (major), and the rhombic signal is attributable to the methoxy $\text{CH}_3\text{O}^\cdot$ radical (minor)—the remaining signal from the methoxy radical is overlapped by the hydroxymethyl radical. A CH bond in CH_3OH can effectively overlap with a lone pair of electrons in the OH oxygen (hyperconjugation). As a result, the oxygen electron pair may activate the CH bond making it reductive. Comparison of the two EPR spectra of the $\text{UO}_2^{2+}-\text{CH}_3\text{OH}-\text{H}_2\text{O}$ mixtures (Fig. 1b and c) also shows that the intensities of both UO_2^+ and $\cdot\text{CH}_2\text{OH}$ signals increased as the concentration of methanol increased, and that as the concentration of CH_3OH in the mixture was increased, the ratio of intensity of $\cdot\text{CH}_2\text{OH}$ signal to intensity of UO_2^+ signal increased.

EPR simulations on Fig. 1 were conducted with EasySpin. Parameters used were: Fig. 1a: ratio of Axial:Rhombic = 1:0.8. Axial: $g_{\parallel} = 2.034$ and $g_{\perp} = 2.016$; broadening: 0.8. Rhombic: $g_x = 2.034$, $g_y = 2.017$, $g_z = 2.002$; broadening: 0.6. Fig. 1c: ratio of Axial:Rhombic = 2:1. Axial: $g_{\parallel} = 2.033$ and $g_{\perp} = 2.016$; broadening: 0.28. Rhombic: $g_x = 2.033$, $g_y = 2.016$, $g_z = 2.002$; broadening: 0.6. The comparison of experimental and simulated EPR spectra of the methanol

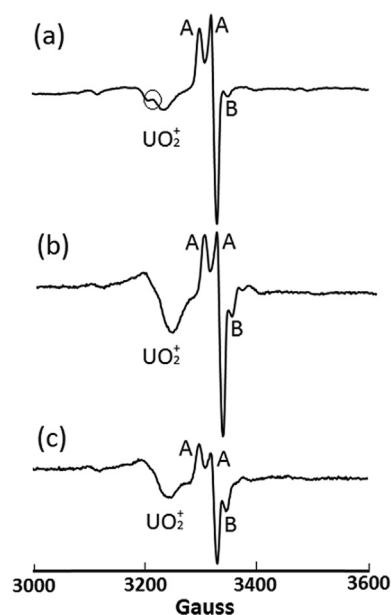


Fig. 1. The EPR spectra of UO_2^{2+} (0.050 M, as the nitrate salt) in (a) anhydrous CH_3OH , (b) the medium with $\text{CH}_3\text{OH}:\text{H}_2\text{O} = 2:1$ (volume ratio), and (c) the medium with $\text{CH}_3\text{OH}:\text{H}_2\text{O} = 1:1$ (volume ratio). UO_2^{2+} was incubated in each medium for 24 h in the dark at room temperature, and then a spectrum recorded in the frozen state at 80 K. The splitting of the UO_2^{2+} signal in (a) is circled. A: The axial signal, assigned to hydroxymethyl $\cdot\text{CH}_2\text{OH}$ radical (major). B: The rhombic signal, assigned to methoxy $\text{CH}_3\text{O}\cdot$ radical (minor).

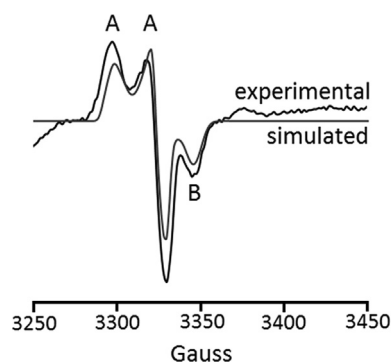


Fig. 2. Comparison of simulated (with flat baseline) and experimental EPR spectra of the hydroxymethyl $\cdot\text{CH}_2\text{OH}$ radical (Signal A) and the methoxy $\text{CH}_3\text{O}\cdot$ radical (Signal B).

radicals ($\cdot\text{CH}_2\text{OH}$ and $\text{CH}_3\text{O}\cdot$) in Fig. 1c is exhibited in Fig. 2, and they are essentially consistent.

The formations of two radicals $\cdot\text{CH}_2\text{OH}$ and $\text{CH}_3\text{O}\cdot$ have been further confirmed by variable power EPR measurements on the mixtures of UO_2^{2+} (0.05 M)– CH_3OH – H_2O with volume ratios of $\text{CH}_3\text{OH}:\text{H}_2\text{O} = 2:1$ and $1:1$, respectively. For both mixtures, the intensities of Signals A and B in the EPR spectra obtained at different microwave powers were determined. The results are included in Fig. 3. Fig. 3 shows that intensities of the axial signal reached maxima (saturation) at the power of 1.5–2.5 mW (Lines 1 and 2). As the power further increased, the intensities decreased. However, the upper-field component (Signal B) was not saturated at 1.5–2.5 mW. Instead, its intensity kept increasing as a function of the power until 20 mW (Line 3). The results have confirmed that the lower-field peak and the derivative (marked with A in Fig. 1) originate from the same radical ($\cdot\text{CH}_2\text{OH}$), while the upper-level component (marked with B in Fig. 1) originates from another radical ($\text{CH}_3\text{O}\cdot$).

The EPR identification of both UO_2^{2+} and $\cdot\text{CH}_2\text{OH}$ (the major radical) from the thermal reaction mixtures of UO_2^{2+} and CH_3OH clearly

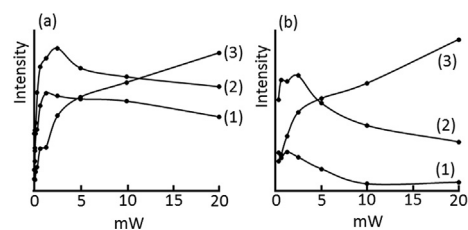


Fig. 3. Variable power EPR measurements for the mixtures of UO_2^{2+} (0.05 M, as the nitrate salt) in the CH_3OH – H_2O solvents with (a) $\text{CH}_3\text{OH}:\text{H}_2\text{O} = 2:1$ (volume ratio), and (b) $\text{CH}_3\text{OH}:\text{H}_2\text{O} = 1:1$ (volume ratio). Each sample was incubated for 24 h in the dark at room temperature. The EPR spectra were then recorded in the frozen state at 80 K with different microwave powers (0–20 mW). The intensities (the signal height) of the lower-field peak (Line 1), first derivative in the middle (Line 2), and upper-field component (Line 3) were measured as a function of the microwave power (mW). Refer to Fig. 1 for the different EPR signals.

shows a charge-transfer process from a CH bond of CH_3OH to the uranium valence shell in UO_2^{2+} to lead to a redox reaction (Eq. (2)).



The minor $\text{CH}_3\text{O}\cdot$ radical is most likely produced by a water catalyzed isomerization of initially formed $\cdot\text{CH}_2\text{OH}$.

Our EPR spectroscopic studies have shown that the UO_2^+ signal generated by reduction of UO_2^{2+} with anhydrous methanol (Fig. 1a) had a splitting, while in the mixed methanol-water solutions the splitting on the UO_2^+ signals was not seen (Fig. 1b and c). Such splitting on the UO_2^+ signals was also observed and became more appreciable in the EPR spectra of the solutions of UO_2^{2+} (as the acetate salt) in the CH_3OH – H_2SO_4 mixtures (the mixtures of anhydrous methanol and 98% H_2SO_4) (Fig. 4). Conceivably, the splitting in the UO_2^+ signals in all the EPR spectra of Figs. 1a and 4 originates possibly from the spin-spin interactions between the unpaired electrons in the two paramagnetic centers, UO_2^+ and $\cdot\text{CH}_2\text{OH}$. The observation of the spin-spin interactions is indicative of the formation of a $[\text{UO}_2^+, \cdot\text{CH}_2\text{OH}]$ ion-radical pair between the two paramagnetic centers in anhydrous methanol. As the content of water in the media became appreciable (e.g. when volume ratio of $\text{CH}_3\text{OH}:\text{H}_2\text{O} = 2:1$ and $1:1$), UO_2^+ and $\cdot\text{CH}_2\text{OH}$ were possibly separated and the spin-spin interactions did not take place.

Fig. 4 also shows that sulfuric acid in the reaction media has led to a substantial increase in the intensity of the upper-level component ($\text{CH}_3\text{O}\cdot$) in the EPR spectra, while in the anhydrous methanol without the acid the upper-level component (Signal B) in the spectrum was tiny (Fig. 1a). The spectral data support a sulfuric-acid-catalyzed isomerization of hydroxymethyl ($\cdot\text{CH}_2\text{OH}$) radical to methoxy ($\text{CH}_3\text{O}\cdot$) radical as shown below (Eq. (3)).

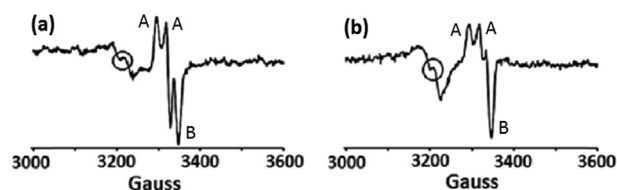


Fig. 4. The EPR spectra of UO_2^+ (broad signals in the left side), the hydroxymethyl $\cdot\text{CH}_2\text{OH}$ radical (axial signals marked with A), and methoxy $\text{CH}_3\text{O}\cdot$ radical (upper-field component marked with B) generated from the mixtures containing UO_2^{2+} (as the acetate salt), anhydrous CH_3OH , and 98% H_2SO_4 after the mixtures were incubated for 24 h in the dark at room temperature. (a) $[\text{UO}_2^{2+}] = 0.05$ M in the CH_3OH – H_2SO_4 (1 M) solution; and (b) $[\text{UO}_2^{2+}] = 0.05$ M in the CH_3OH – H_2SO_4 (2 M) solution. The circled areas in the UO_2^+ signals indicate the splitting reasonably due to the spin-spin interactions between UO_2^+ and $\cdot\text{CH}_2\text{OH}$.

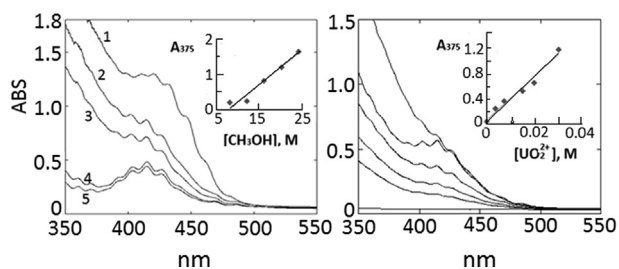
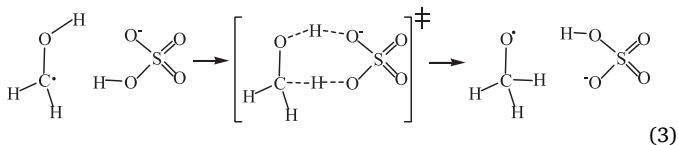


Fig. 5. Left: The UV-Vis spectra of initial mixtures of UO_2^{2+} (0.05 M, as the nitrate salt) with methanol and water. (1) Anhydrous CH_3OH ($[\text{CH}_3\text{OH}] = 24.7 \text{ M}$); (2) volume ratio $\text{CH}_3\text{OH}:\text{H}_2\text{O} = 5:1$ ($[\text{CH}_3\text{OH}] = 20.6 \text{ M}$); (3) volume ratio $\text{CH}_3\text{OH}:\text{H}_2\text{O} = 2:1$ ($[\text{CH}_3\text{OH}] = 16.4 \text{ M}$); (4) volume ratio $\text{CH}_3\text{OH}:\text{H}_2\text{O} = 1:1$ ($[\text{CH}_3\text{OH}] = 12.3 \text{ M}$); and (5) volume ratio $\text{CH}_3\text{OH}:\text{H}_2\text{O} = 1:2$ ($[\text{CH}_3\text{OH}] = 8.2 \text{ M}$). ($A_{375} = 0.0927[\text{CH}_3\text{OH}] - 0.0704$, $R^2 = 0.962$); **Right:** The UV-Vis spectra of UO_2^{2+} with different molar concentrations in the mixed methanol–water solutions with the volume ratio of $\text{CH}_3\text{OH}:\text{H}_2\text{O} = 5:1$. Each spectrum was recorded immediately after a mixture was made. From the bottom to top, $[\text{UO}_2^{2+}] = 0 \text{ M}$, 0.00375 M , 0.0075 M , 0.015 M , 0.020 M , and 0.030 M . ($A_{375} = 34.60[\text{UO}_2^{2+}] + 0.061$, $R^2 = 0.968$).

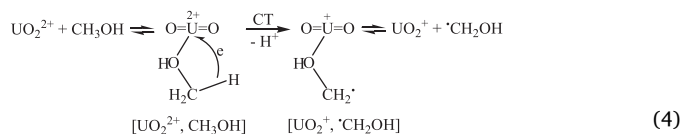


H_2SO_4 is ionized to HSO_4^- in methanol. HSO_4^- then relays a concerted proton transfer from oxygen to carbon in $\cdot\text{CH}_2\text{OH}$, resulting in isomerization of $\cdot\text{CH}_2\text{OH}$ to $\cdot\text{CH}_3\text{O}$. This mechanism is comparable with a recent theoretical study on the isomerization between different methanol radicals [14].

We further characterized the charge-transfer reduction of UO_2^{2+} with CH_3OH by UV-Vis spectroscopy. The UV-Vis spectra of UO_2^{2+} (as the nitrate salt) in both anhydrous methanol and in the methanol–water mixtures exhibited strong broad absorptions at 350–400 nm (Fig. 5). The absorption bands centered at $\sim 420 \text{ nm}$ in the spectra of samples containing lower concentrations of methanol and higher concentrations of water (the bottom two curves in Fig. 5-left) originate from the promotion of an electron from an axial oxygen 2p orbital to a uranium (VI) 5f nonbonding orbital with vibrational fine structure resolved [15,16]. Fig. 5-left shows that the intensity of the absorptions at 350–400 nm (represented by A_{375} , the absorbance at 375 nm) is directly proportional to the molar concentration of methanol ($[\text{CH}_3\text{OH}]$, M) in the $\text{CH}_3\text{OH}-\text{H}_2\text{O}$ mixtures at a fixed uranyl (VI) concentration ($[\text{UO}_2^{2+}] = 0.050 \text{ M}$). Fig. 5-right shows that the intensity of the absorptions A_{375} is also directly proportional to the molar concentration of UO_2^{2+} ($[\text{UO}_2^{2+}]$, M) in the $\text{UO}_2^{2+}-\text{CH}_3\text{OH}-\text{H}_2\text{O}$ solutions with a fixed volume ratio of $\text{CH}_3\text{OH}:\text{H}_2\text{O} = 5:1$. The quantitative linear relationships between A_{375} and $[\text{CH}_3\text{OH}]$ and between A_{375} and $[\text{UO}_2^{2+}]$ show that the absorption at 350–400 nm involves both a UO_2^{2+} cation and a CH_3OH molecule and originates from a 1:1 EDA [UO_2^{2+} , CH_3OH] complex (formed reversibly by interaction of UO_2^{2+} and CH_3OH) as a result of a single-electron transfer from a CH bond in CH_3OH (electron-donor) to the uranium valence shell of UO_2^{2+} (electron acceptor) within the [UO_2^{2+} , CH_3OH] complex. Its absorbance is directly proportional to concentrations of both uranyl (VI) and methanol, being consistent with the equilibrium for the formation of the EDA complex. The features of high intensity and a band being very broad for the absorption are also characteristic of intermolecular charge-transfer absorptions. The single-electron transfer, which can take place photochemically as well as thermally in the ground state, gives rise to formations of both UO_2^+ and $\cdot\text{CH}_2\text{OH}$ (identified by EPR) in the $\text{UO}_2^{2+}-\text{CH}_3\text{OH}-\text{H}_2\text{O}$ solutions. The charge-transfer absorptions of the $\text{UO}_2^{2+}-\text{CH}_3\text{OH}-\text{H}_2\text{O}$ solutions are similar to those for the $\text{UO}_2^{2+}-\text{X}^--\text{H}_2\text{O}$ ($\text{X}^- = \text{Br}^-$ and I^-) solutions we observed before [2].

Very recently, charge-transfer absorptions for the $\text{UO}_2^{2+}-\text{Cl}^--\text{H}_2\text{O}$ solutions have been observed at elevated temperatures up to 250°C , showing their intensities were enhanced by increasing temperature [17].

Previous investigations have shown that the OH group in an alcohol (e.g. ethanol and PVA) can coordinate to the uranium center of UO_2^{2+} in the equatorial positions forming a uranyl–alcohol adduct [3,18]. By its nature, the EDA complex [UO_2^{2+} , CH_3OH] that we have observed from the above UV-Vis study could be such a uranyl–alcohol adduct. We believe that within this EDA complex, a single-electron transfer between a methanol CH bond and the uranium center of UO_2^{2+} (an inner-sphere charge-transfer) possibly occurs leading to the formation of an ion-radical [UO_2^+ , $\text{HOCH}_2\cdot$] pair (adduct) via the same oxygen \rightarrow uranium coordination bond. Formation of a [UO_2^+ , $\text{HOCH}_2\cdot$] adduct (ion-radical pair) is comparable to the connection of UO_2^+ to the OH groups in PVA radical ($-\text{CH}_2-\text{C}(\text{OH})-\text{CH}_2-$) produced from the γ -ray induced photochemical reduction of UO_2^{2+} by PVA [3]. The overall possible mechanism for the thermal charge-transfer reduction of UO_2^{2+} by CH_3OH is illustrated in the following scheme (Eq. (4)).



First, the hydroxyl $-\text{OH}$ in methanol interacts with uranium in UO_2^{2+} to form an EDA complex [UO_2^{2+} , CH_3OH] via a weak oxygen \rightarrow uranium coordination bond. The reversible formation of [UO_2^{2+} , CH_3OH] is followed by an irreversible charge-transfer within the EDA complex to lead to an ion-radical pair [UO_2^+ , $\cdot\text{CH}_2\text{OH}$] (adduct). We believe that the spin-spin interactions between UO_2^+ and $\cdot\text{CH}_2\text{OH}$ evidenced by EPR spectroscopy (Figs. 1 and 4) in anhydrous methanol take place within the ion-radical pair. In anhydrous methanol, the ion-radical pair is stable and its dissociation is unfavorable. As the content of water in the solution increases, the $\cdot\text{CH}_2\text{OH}$ ligand coordinating to the uranium center in UO_2^+ can be effectively displaced by the H_2O molecules, and the [UO_2^+ , $\text{HOCH}_2\cdot$] adduct dissociates to UO_2^+ (subsequently hydrated) and the discrete $\cdot\text{CH}_2\text{OH}$ radical (Eq. (5)).



As a result, the splitting in the UO_2^+ signal (spin-spin interaction) disappears.

We performed a photochemical reaction of UO_2^{2+} with CH_3OH by irradiating a mixture of UO_2^{2+} (0.05 M, as the nitrate salt) and anhydrous methanol with a mercury lamp (350 nm). Then the reaction mixture was characterized by EPR spectroscopy in the frozen state at 80 K (Fig. 6), showing signals of both $\cdot\text{CH}_2\text{OH}$ (axial signal) and $\text{CH}_3\text{O}\cdot$ (rhombic signal), but no UO_2^+ signal was observed. The lack of UO_2^+ is consistent with the previous investigations on bleaching of the uranyl

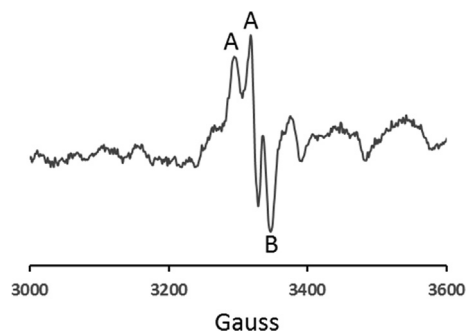


Fig. 6. The EPR spectrum of a mixture of UO_2^{2+} (0.05 M, as the nitrate salt) and anhydrous methanol recorded in the frozen state at 80 K after the mixture was irradiated by a mercury lamp (350 nm) for 30 min at room temperature. A: Axial signal assigned to hydroxymethyl $\cdot\text{CH}_2\text{OH}$ radical. B: Rhombic signal assigned to methoxy $\text{CH}_3\text{O}\cdot$ radical. The UO_2^+ signal is not observed.

(VI) excited state (UO_2^{2+})^{*} by CH_3OH , for which $\cdot\text{CH}_2\text{OH}$ was identified experimentally, but UO_2^+ was not [7]. By comparison with the thermal reduction of UO_2^{2+} with CH_3OH in the dark, we have reinforced that the lack of UO_2^+ in photochemical reactions is due to a facile disproportionation of the initially formed UO_2^+ to UO_2^{2+} and U^{4+} in the light [7,9]. Alternatively, the more recent research has suggested that UO_2^+ may also be oxidized back to UO_2^{2+} photochemically by the O_2 dissolved in the solvent in the presence of the UV light [19,20]. By comparison with the thermal reaction of UO_2^{2+} with CH_3OH which essentially gave $\cdot\text{CH}_2\text{OH}$ (Fig. 1a), we believe that the initially formed $\cdot\text{CH}_2\text{OH}$ underwent subsequent photochemical isomerization to $\text{CH}_3\text{O}\cdot$ likely catalyzed by the methanol solvent molecule (Eq.6).



The formation of $\text{CH}_3\text{O}\cdot$ on flash photolysis of the UO_2^{2+} – CH_3OH mixtures was not found previously [7,9]. We are here reporting the substantial photochemical isomerization of $\cdot\text{CH}_2\text{OH}$ to $\text{CH}_3\text{O}\cdot$ for the first time.

3.2. Thermal charge-transfer reduction of uranyl UO_2^{2+} (VI) to UO_2^+ (V) by ethanol, 2-propanol, and cyclohexanol, and the variable power EPR studies of α -hydroxyalkyl and alkoxy radicals

We characterized the reaction mixtures of UO_2^{2+} (0.05 M, as the nitrate salt) with anhydrous ethanol, and with ethanol and water (volume ratio EtOH:H₂O = 1:1) by EPR (Fig. 7a and b) after the mixtures were incubated at room temperature in the dark for 24 h. We also measured the EPR spectra (Fig. 7c and d) of mixtures of UO_2^{2+} (0.05 M, as the acetate salt) with anhydrous ethanol and 98% sulfuric acid, with overall molar concentrations of H_2SO_4 in the media being 1 M and 2 M respectively, after the mixtures were incubated at room temperature in the dark for 24 h. Both Figs. 7a and b showed strong axial signals (Signals A) analogous to that of the UO_2^{2+} – CH_3OH mixture (Fig. 1a). The signals are attributable to the α -hydroxyethyl $\text{CH}_3\cdot\text{CHOH}$ radical. The UO_2^+ signal is either not observed (Fig. 7a) or very weak (Fig. 7b). Fig. 7c shows that when $[\text{H}_2\text{SO}_4] = 1 \text{ M}$ in the medium, a broad UO_2^+ signal and a stronger rhombic signal (Signal B) were observed in addition to an axial signal (Signal A, $\text{CH}_3\cdot\text{CHOH}$). As the concentration of H_2SO_4 increased to 2 M, the UO_2^+ signal disappeared presumably due to disproportionation of the initially formed UO_2^+ to UO_2^{2+} and U^{4+} . Strong rhombic signals were also observed (Fig. 7d). By analogy to the UO_2^{2+} – CH_3OH system (Fig. 4), the higher-field portion of the rhombic

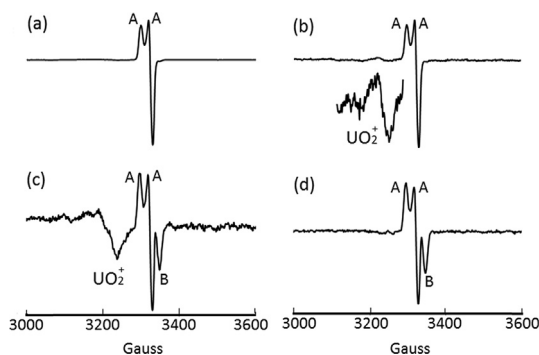


Fig. 7. The EPR spectra of (a) UO_2^{2+} (0.050 M, as the nitrate salt) in anhydrous $\text{CH}_3\text{CH}_2\text{OH}$, (b) UO_2^{2+} (0.050 M, as the nitrate salt) in the medium with $\text{CH}_3\text{CH}_2\text{OH}:\text{H}_2\text{O} = 1:1$ (volume ratio), (c) UO_2^{2+} (0.050 M, as the acetate salt) in the mixture of anhydrous $\text{CH}_3\text{CH}_2\text{OH}$ and 98% H_2SO_4 with $[\text{H}_2\text{SO}_4] = 1.0 \text{ M}$, and (d) UO_2^{2+} (0.050 M, as the acetate salt) in the mixture of anhydrous $\text{CH}_3\text{CH}_2\text{OH}$ and 98% H_2SO_4 with $[\text{H}_2\text{SO}_4] = 2.0 \text{ M}$. Each sample was incubated for 24 h in the dark at room temperature, and then a spectrum recorded in the frozen state at 80 K. The UO_2^+ signal in (b) is enlarged. A: Axial signal assigned to α -hydroxyethyl $\text{CH}_3\cdot\text{CHOH}$ radical. B: Rhombic signal assigned to ethoxy $\text{CH}_3\text{CH}_2\text{O}\cdot$ radical.

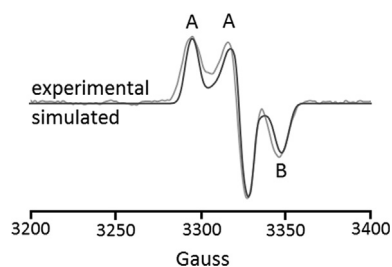
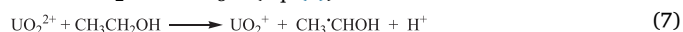


Fig. 8. Comparison of simulated (darker, with flat baseline) and experimental (lighter) EPR spectra of the α -hydroxyethyl $\text{CH}_3\cdot\text{CHOH}$ radical (Signal A) and the ethoxy $\text{CH}_3\text{CH}_2\text{O}\cdot$ radical (Signal B).

signal (B) observed in Fig. 7c and d is attributable to the ethoxy $\text{CH}_3\text{CH}_2\text{O}\cdot$ radical.

The experimental EPR spectrum in Fig. 7d has been simulated (Fig. 8). The simulation shows that the g-values for the axial signal (Signal A, $\text{CH}_3\cdot\text{CHOH}$) are $g_{\parallel} = 2.033$ and $g_{\perp} = 2.014$ with broadening 0.52, and the g-values for the rhombic signal (Signal B, $\text{CH}_3\text{CH}_2\text{O}\cdot$) are $g_x = 2.033$, $g_y = 2.017$, and $g_z = 2.001$ with broadening 0.52. The ratio of axial to rhombic signal is 2:9. Fig. 8 shows that the simulated and experimental spectra are essentially consistent.

The EPR data has indicated that there was a thermal charge-transfer redox reaction between UO_2^{2+} and $\text{CH}_3\text{CH}_2\text{OH}$ to give UO_2^+ and $\text{CH}_3\cdot\text{CHOH}$ (Eq. (7)), and in the presence of H_2SO_4 some α -hydroxyethyl $\text{CH}_3\cdot\text{CHOH}$ radical isomerizes to the ethoxy $\text{CH}_3\text{CH}_2\text{O}\cdot$ radical partially (Eq. 8), following the same mechanism as that for isomerization of $\cdot\text{CH}_2\text{OH}$ to $\text{CH}_3\text{O}\cdot$ (Eq. (3)).



The thermal (in the dark) and photochemical (with Hg UV lamp) reactions of UO_2^{2+} (as the nitrate salt) with 2-propanol ($(\text{CH}_3)_2\text{CHOH}$) were conducted at room temperature and the products were identified by EPR spectroscopy. Since both solubility of UO_2^{2+} in $(\text{CH}_3)_2\text{CHOH}$ and solubility of $(\text{CH}_3)_2\text{CHOH}$ in water are low, the reactions were performed in the liquid acetone media, with volume ratio of 2-propanol:acetone = 1:1. An EPR spectrum (Fig. 9a) was recorded on a frozen mixture of UO_2^{2+} (0.05 M)–2-propanol–acetone at 80 K after the mixture was incubated in the dark at room temperature for 24 h. The spectrum exhibited a weak broad UO_2^+ signal and a strong axial signal. By analogy to the spectra of UO_2^{2+} – CH_3OH and UO_2^{2+} – $\text{CH}_3\text{CH}_2\text{OH}$ systems, the axial signal is attributable to the α -hydroxyl-2-propyl $(\text{CH}_3)_2\text{C}\cdot\text{OH}$ radical. Fig. 9b shows the EPR spectrum of a frozen mixture of UO_2^{2+} (0.05 M)–2-propanol–acetone at 80 K after the mixture was irradiated by a Hg UV-lamp (350 nm) for 0.5 h at room temperature. A broad UO_2^+ signal was observed clearly. A moderately strong upper-field portion of the rhombic signal is apparent. The rhombic signal is attributable to the 2-propyl $(\text{CH}_3)_2\text{CH}\cdot\text{O}$ radical by comparison to the equivalent signal in Figs. 1, 6, and 7.

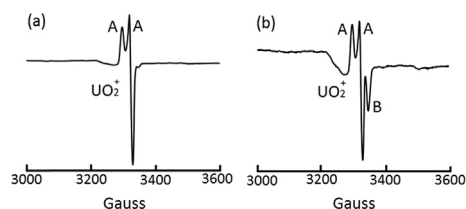
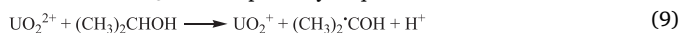


Fig. 9. The EPR spectra of UO_2^{2+} (0.050 M, as the nitrate salt) in a mixture of 2-propanol (i-PrOH) and acetone with i-PrOH:acetone = 1:1 (volume ratio) recorded in the frozen state at 80 K (a) after the mixture was incubated for 24 h in the dark at room temperature; and (b) after the mixture was irradiated by a mercury lamp (350 nm) for 0.5 h at room temperature. A: Axial signal assigned to α -hydroxyl-2-propyl $(\text{CH}_3)_2\text{C}\cdot\text{OH}$ radical. B: Rhombic signal assigned to 2-propoxy $(\text{CH}_3)_2\text{CH}\cdot\text{O}$ radical.

Fig. 9b has been simulated, with ratio of axial to rhombic signal being 1:5. The g -values of axial signal are $g_{\parallel} = 2.033$ and $g_{\perp} = 2.017$. The g -values of rhombic signal are $g_x = 2.033$, $g_y = 2.017$, and $g_z = 2.002$. The broadening is 0.4 for both axial and rhombic signals. Similar to the simulations of Figs. 1c and 7d, the simulated spectrum for Fig. 9b is essentially consistent with the experimental spectrum.

The EPR data indicate that UO_2^{2+} and $(\text{CH}_3)_2\text{CHOH}$ underwent both thermal and photochemical charge-transfer redox reactions to give UO_2^+ and $(\text{CH}_3)_2\text{C}\cdot\text{OH}$ (Eq. (9)). In the light, some $(\text{CH}_3)_2\text{C}\cdot\text{OH}$ isomerized to $(\text{CH}_3)_2\text{CH}\cdot\text{O}$ partially (Eq. (10)).



The photochemical isomerization (Eq.10) is catalyzed by $(\text{CH}_3)_2\text{CHOH}$, and it reinforces the analogous methanol-catalyzed photochemical isomerization of $\cdot\text{CH}_2\text{OH}$ to $\text{CH}_3\cdot\text{O}$ (Eq. (6)). Most likely, the 2-propanol-catalyzed photochemical isomerization of $(\text{CH}_3)_2\text{C}\cdot\text{OH}$ to $(\text{CH}_3)_2\text{CH}\cdot\text{O}$ follows the same mechanism as that of the methanol-catalyzed photochemical isomerization of $\cdot\text{CH}_2\text{OH}$ to $\text{CH}_3\cdot\text{O}$.

Variable power EPR measurements were conducted on a thermal reaction mixture of UO_2^{2+} - $\text{CH}_3\text{CH}_2\text{OH}$ - H_2SO_4 (1 M) and a photochemical reaction mixture of UO_2^{2+} - $(\text{CH}_3)_2\text{CHOH}$ -acetone. For both systems, the EPR spectra exhibited several signals (Figs. 7c and 9b). The intensity of each signal was determined at different microwave powers. The results are included in Fig. 10. Fig. 10a (the UO_2^{2+} - $\text{CH}_3\text{CH}_2\text{OH}$ - H_2SO_4 mixture) shows that intensities of both the lower-field peak and middle spectral component reached a maxima (saturation) at the power of 1.5 mW (Lines 1 and 3). As the power further increased, the intensities decreased. However, the upper-field signal was not saturated at 1.5 mW. Instead, its intensity kept increasing as a function of the power until 8 mW (Line 2). Fig. 10b (the UO_2^{2+} - $(\text{CH}_3)_2\text{CHOH}$ -acetone mixture) shows that intensities of the axial system reached its maximum (saturation) at the power of 1.3 mW (Lines 1 and 3). As the power further increased, the intensities decreased. However, the upper-field portion of the rhombic signal was not saturated (maximum intensity) until the power reached 4–5 mW (Line 2). The results have confirmed that the axial signal A (the lower-level peak and middle component) in each spectrum originates from the same α -hydroxyalkyl ($\text{CH}_3\cdot\text{CHOH}$ or $(\text{CH}_3)_2\text{C}\cdot\text{OH}$) radical, while the upper-level portion of rhombic signal (B) originates from another alkoxy ($\text{CH}_3\text{CH}_2\cdot\text{O}$ or $(\text{CH}_3)_2\text{CH}\cdot\text{O}$) radical. The variable power EPR measurements for all the UO_2^{2+} -alcohol (methanol, ethanol, and 2-propanol) mixtures are consistent, supporting the assignment of the axial signals to an α -hydroxyalkyl radical and the assignment of the rhombic signal to an alkoxy radical.

The thermal reaction of UO_2^{2+} with cyclohexanol was performed by

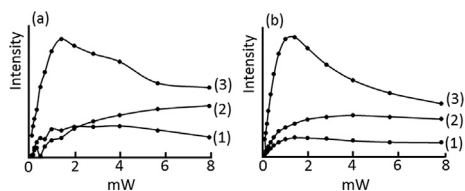


Fig. 10. Variable power EPR measurements for (a) UO_2^{2+} (0.050 M, as the acetate salt) in the mixture of anhydrous $\text{CH}_3\text{CH}_2\text{OH}$ and 98% H_2SO_4 with $[\text{H}_2\text{SO}_4] = 1.0$ M after the sample incubated for 24 h in the dark at room temperature, and (b) UO_2^{2+} (0.050 M, as the nitrate salt) in the mixture of 2-propanol (i-PrOH) and acetone with i-PrOH:acetone = 1:1 (volume ratio) after the sample irradiated by a mercury lamp (350 nm) for 0.5 h at room temperature. For each sample, the EPR spectra were recorded in the frozen state at 80 K with different microwave powers (0–8 mW). The intensities (the signal height) of the lower-field component (Line 1), upper-field component (Line 2), and middle spectral component (Line 3) were measured as a function of the microwave power (mW). Refer to Fig. 7c (UO_2^{2+} - $\text{CH}_3\text{CH}_2\text{OH}$ - H_2SO_4) and Fig. 9b (UO_2^{2+} -i-PrOH-acetone) for the different EPR signals.

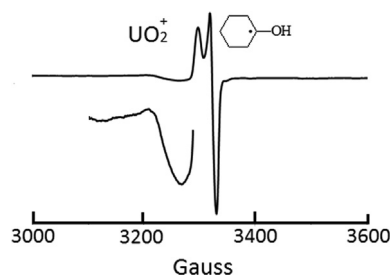
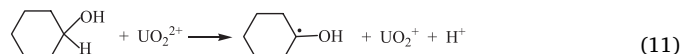


Fig. 11. The EPR spectrum of a mixture of UO_2^{2+} (0.05 M, as the nitrate salt) and cyclohexanol (0.30 M) in acetone recorded in the frozen state at 80 K after the sample was incubated for 24 h in the dark at room temperature. The broad UO_2^+ signal is enlarged.

incubating a mixture of UO_2^{2+} (0.05 M, as the nitrate salt) and cyclohexanol (0.3 M) in liquid acetone in the dark at room temperature for 24 h. Then an EPR spectrum was recorded on the frozen reaction mixture at 80 K (Fig. 11). A weak UO_2^+ signal and an axial signal were observed, which were attributed to the α -hydroxycyclohexyl radical. The spectral data shows that a thermal charge-transfer reduction of UO_2^{2+} by cyclohexanol has taken place to give UO_2^+ and α -hydroxycyclohexyl radical (Eq. (11)).



Although we have got EPR evidence for the spin-spin interactions between UO_2^+ and hydroxymethyl $\cdot\text{CH}_2\text{OH}$ radical, no evidence for the spin-spin interactions between UO_2^+ and other α -hydroxyalkyl (α -hydroxyethyl, α -hydroxyl-2-propyl, and α -hydroxycyclohexyl) radicals was found in this research.

We further characterized the charge-transfer reduction of UO_2^{2+} with ethanol, 2-propanol, and cyclohexanol by UV-Vis spectroscopy. Similar to the UO_2^{2+} - CH_3OH - H_2O mixtures, the UV-Vis spectra of UO_2^{2+} (0.05 M, as the nitrate salt) in the mixtures containing ethanol, 2-propanol, and cyclohexanol exhibited strong broad absorptions at 350–400 nm (Fig. 12). The absorption bands centered at ~ 420 nm in the spectra of samples containing lower concentrations of the alcohols originate from the promotion of an electron from a UO_2^{2+} axial oxygen 2p orbital to a uranium (VI) 5f nonbonding orbital [15,16]. As the concentration of the alcohol increased in each sample, a strong absorption evolved at 350–400 nm, with A_{375} (the absorbance at 375 nm) being directly proportional to the molar concentration of the alcohol. By comparison to the spectra of the UO_2^{2+} - CH_3OH - H_2O mixtures, the

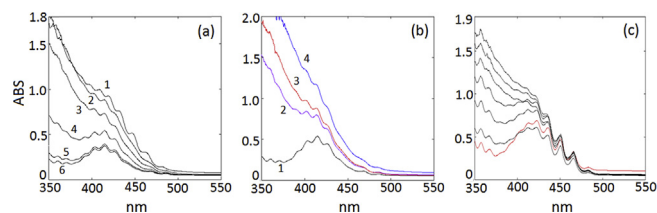


Fig. 12. (a) The UV-Vis spectra of initial mixtures of UO_2^{2+} (0.05 M, as the nitrate salt) with ethanol and water. (1) Anhydrous $\text{CH}_3\text{CH}_2\text{OH}$ ($[\text{CH}_3\text{CH}_2\text{OH}] = 17.1$ M); (2) volume ratio $\text{CH}_3\text{CH}_2\text{OH}:\text{H}_2\text{O} = 5:1$ ($[\text{CH}_3\text{CH}_2\text{OH}] = 14.3$ M); (3) volume ratio $\text{CH}_3\text{CH}_2\text{OH}:\text{H}_2\text{O} = 2:1$ ($[\text{CH}_3\text{CH}_2\text{OH}] = 11.4$ M); (4) volume ratio $\text{CH}_3\text{CH}_2\text{OH}:\text{H}_2\text{O} = 1:1$ ($[\text{CH}_3\text{CH}_2\text{OH}] = 8.6$ M); (5) volume ratio $\text{CH}_3\text{CH}_2\text{OH}:\text{H}_2\text{O} = 1:2$ ($[\text{CH}_3\text{CH}_2\text{OH}] = 5.7$ M); and (6) volume ratio $\text{CH}_3\text{CH}_2\text{OH}:\text{H}_2\text{O} = 1:5$ ($[\text{CH}_3\text{CH}_2\text{OH}] = 2.9$ M). ($A_{375} = 0.095[\text{EtOH}] - 0.19$, $R^2 = 0.925$). (b) The UV-Vis spectra of initial mixtures of UO_2^{2+} (0.05 M, as the nitrate salt) with 2-propanol (i-PrOH) and water. (1) Pure H_2O ($[\text{i-PrOH}] = 0$ M); (2) $[\text{i-PrOH}] = 0.13$ M; (3) $[\text{i-PrOH}] = 0.26$ M; and (4) $[\text{i-PrOH}] = 0.52$ M. ($A_{375} = 3.10[\text{i-PrOH}] + 0.43$, $R^2 = 0.926$). (c) The UV-Vis spectra of initial mixtures of UO_2^{2+} (0.05 M, as the nitrate salt) with cyclohexanol and acetone. From bottom to top, $[\text{cyclohexanol}] = 0$ M, 0.25 M, 0.50 M, 1.0 M, 1.5 M, 2.0 M, and 2.5 M. ($A_{375} = 0.451[\text{ROH}] + 0.370$, $R^2 = 0.96$).

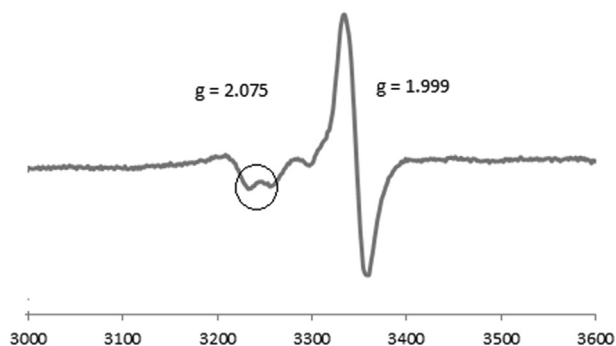


Fig. 13. The EPR spectrum of a mixture of UO_2^{2+} (0.05 M, as the nitrate salt) and diphenyl sulfide Ph_2S (0.25 M) in liquid acetone recorded in the frozen state at 80 K after the sample was incubated for 24 h in the dark at room temperature. The spectrum exhibits UO_2^+ ($g = 2.075$) and $\text{Ph}_2\text{S}^{\cdot+}$ ($g = 1.999$). The circled area shows splitting of the UO_2^+ signal.

absorption at 350–400 nm is due to a 1:1 EDA [UO_2^{2+} , ROH] complex (ROH = ethanol, 2-propanol, or cyclohexanol) as a result of a single-electron transfer from an α -CH bond in ROH to the uranium valence shell of UO_2^{2+} within the [UO_2^{2+} , ROH] complex. The single-electron transfer, which can take place photochemically as well as thermally in the ground state, gives rise to the formations of both UO_2^+ and an α -hydroxyalkyl radical (identified by EPR) in the UO_2^{2+} -alcohol mixtures.

3.3. Thermal charge-transfer reduction of uranyl UO_2^{2+} (VI) to UO_2^+ (V) by diphenyl sulfide (Ph_2S), and evidence for spin-spin interactions between UO_2^+ (V) and diphenyl sulfide radical cation ($\text{Ph}_2\text{S}^{\cdot+}$)

Photolytic studies of the reaction of UO_2^{2+} and diaryl sulfides (R_2S) have shown that R_2S can be oxidized by the excited (UO_2^{2+})* in the UV light to a cationic diaryl sulfide radical $\text{R}_2\text{S}^{\cdot+}$, but no reduced uranium species was observed experimentally [8,21]. In the present work, we have carried out the redox reaction of UO_2^{2+} and Ph_2S thermally in the dark at normal room temperature and then characterized the reaction products by EPR spectroscopy. Fig. 13 shows the EPR spectrum of a reaction mixture of UO_2^{2+} (as the nitrate salt) and Ph_2S in liquid acetone that was incubated in the dark at ambient temperature for 24 h. Both UO_2^+ ($g = 2.075$) and the $\text{Ph}_2\text{S}^{\cdot+}$ radical cation ($g = 1.999$) were observed, showing that a single-electron transfer took place from Ph_2S (electron donor) to UO_2^{2+} (electron acceptor) to lead to an oxidation-reduction reaction (Eq. (12)).



Similar to the reduction of UO_2^{2+} by anhydrous methanol, the EPR spectrum of the UO_2^{2+} - Ph_2S -acetone mixture (Fig. 13) exhibited splitting on the UO_2^+ signal, suggesting the spin-spin interaction between UO_2^+ and $\text{Ph}_2\text{S}^{\cdot+}$. Most likely, such an interaction occurs between the unpaired electrons of UO_2^+ and $\text{Ph}_2\text{S}^{\cdot+}$ within a [UO_2^+ , $\text{Ph}_2\text{S}^{\cdot+}$] ion-radical pair.

The thermal charge-transfer redox between UO_2^{2+} and Ph_2S has been further studied in this work by UV-Vis spectroscopy. Fig. 14-left shows the UV-Vis spectra of the initial mixtures of UO_2^{2+} (0.05 M, as the nitrate salt) and various concentrations of Ph_2S in liquid acetone. All the spectra exhibited a broad band with the maximum absorption being at ~ 420 nm. It is due to the transfer of an electron from a UO_2^{2+} axial oxygen 2p orbital to a uranium (VI) 5f nonbonding orbital [15,16]. In addition, a strong absorption at 350–400 nm evolved as the concentration of Ph_2S increased gradually. The intensity of the absorption at 350–400 nm (represented by the absorbance A_{375} at 375 nm) was shown to be directly proportional to the molar concentration of Ph_2S at a fixed concentration of UO_2^{2+} (0.05 M). We also recorded the UV-vis spectra of the initial UO_2^{2+} - Ph_2S (1.4 M)-acetone mixtures with variable concentrations of UO_2^{2+} (Fig. 14-right) and

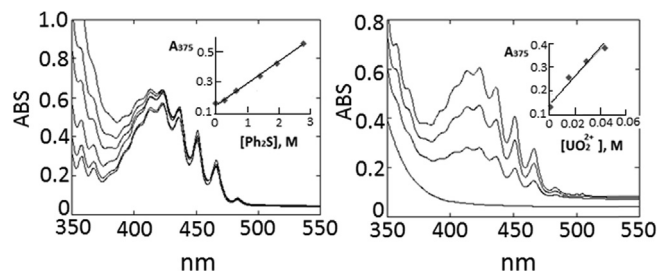
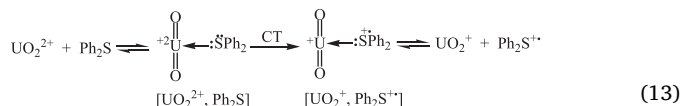


Fig. 14. Left: The UV-Vis spectra of UO_2^{2+} (0.05 M, as the nitrate salt) in the mixtures of diphenyl sulfide (Ph_2S) and liquid acetone. Each spectrum was recorded immediately after the sample was made. From the bottom to top, $[\text{Ph}_2\text{S}] = 0$ M, 0.271 M, 0.649 M, 1.42 M, 1.94 M, and 2.80 M. ($A_{375} = 0.138[\text{Ph}_2\text{S}] + 0.159$, $R^2 = 0.998$); Right: The UV-Vis spectra of UO_2^{2+} in different molar concentrations in the Ph_2S -acetone solutions with the $[\text{Ph}_2\text{S}] = 1.42$ M. Each spectrum was recorded immediately after the sample was made. From the bottom to top, $[\text{UO}_2^{2+}] = 0$ M, 0.015 M, 0.030 M, and 0.045 M. ($A_{375} = 5.533[\text{UO}_2^{2+}] + 0.151$, $R^2 = 0.960$).

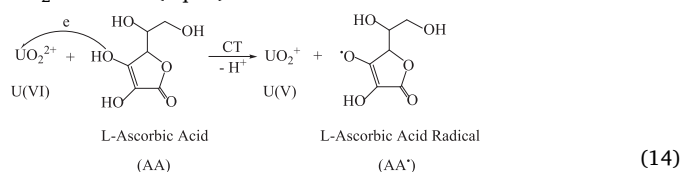
found that A_{375} is directly proportional to molar concentration of UO_2^{2+} as well as at a fixed concentration of Ph_2S (1.4 M). The linear relationships between A_{375} and $[\text{Ph}_2\text{S}]$ (molarity) and between A_{375} and $[\text{UO}_2^{2+}]$ (molarity) indicate the reversible formation of a 1:1 charge-transfer complex [UO_2^{2+} , Ph_2S] and the absorption at 350–400 nm originates from a single-electron transfer from sulfur in Ph_2S (electron donor) to the uranium center in UO_2^{2+} (electron acceptor) within the EDA [UO_2^{2+} , Ph_2S] complex to give UO_2^+ and $\text{Ph}_2\text{S}^{\cdot+}$ (Eq. (13)).



The absorbance for this absorption is directly proportional to concentrations of both UO_2^{2+} and Ph_2S , being consistent with the equilibrium for the formation of the EDA [UO_2^{2+} , Ph_2S] complex. Analogous to the [UO_2^{2+} , CH_3OH] complex, the EDA complex [UO_2^{2+} , Ph_2S] is reasonably formed reversibly via an S \rightarrow U coordination bond. Then an irreversible single-electron transfer from sulfur of Ph_2S to the uranium center of UO_2^{2+} occurs within the [UO_2^{2+} , Ph_2S] complex to lead to an ion-radical pair [UO_2^+ , $\text{Ph}_2\text{S}^{\cdot+}$] which has been identified by EPR. The ion-radical pair can undergo a reversible dissociation to separate UO_2^+ and $\text{Ph}_2\text{S}^{\cdot+}$. However, in our experimental conditions, the dissociation seems unfavorable. Direct identification of both UO_2^+ and $\text{Ph}_2\text{S}^{\cdot+}$ by EPR from a mixture of UO_2^{2+} and Ph_2S , together with the UV-Vis study, has confirmed the above overall charge-transfer mechanism in the ground state (Eq. 13).

3.4. Thermal charge-transfer reduction of uranyl UO_2^{2+} (VI) to UO_2^+ (V) by L-ascorbic acid

L-Ascorbic acid (AA) is a biologically relevant antioxidant (reductant). We carried out a thermal reduction of UO_2^{2+} (0.05 M, as the acetate salt) by AA (0.5 M) in aqueous H_2SO_4 (0.5 M) solution. The reaction mixture was incubated in the dark at ambient temperature for 24 h. The resulting EPR spectrum (Fig. 15a) showed a broad signal of UO_2^+ ($g = 2.07$) and a strong sharp singlet signal ($g = 2.00$) attributable to the L-ascorbic acid radical (AA \cdot). The result revealed a charge-transfer redox reaction between UO_2^{2+} and AA effected by transfer of a single-electron from an OH group of AA to uranium in UO_2^{2+} to give UO_2^+ and AA \cdot (Eq. 14).



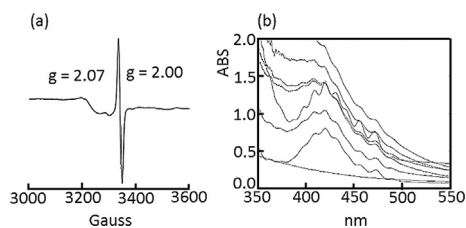
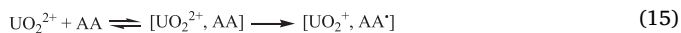


Fig. 15. (a) The EPR spectrum of a mixture of UO_2^{2+} (0.05 M, as the acetate salt) and ascorbic acid (AA, 0.5 M) in aqueous sulfuric acid (0.5 M) recorded in the frozen state at 80 K after the sample was incubated for 24 h in the dark at room temperature. The spectrum exhibits UO_2^+ ($g = 2.07$) and ascorbic acid radical AA' ($g = 2.00$). (b) The UV-Vis spectra of the initial mixtures of UO_2^{2+} (0.05 M, as the acetate salt) and L-ascorbic acid (AA) in different concentrations in aqueous H_2SO_4 (0.5 M). From the bottom to top, $[\text{AA}] = 1.0$ M (without UO_2^{2+}), 0.05 M, 0.2 M, 0.3 M, 0.4 M, 0.5 M, 0.7 M, and 1.0 M. ($A_{375} = 2.01[\text{AA}] + 0.41$, $R^2 = 0.93$).

The unpaired electron in AA' can be possibly strongly attracted to the uranium valence shell of UO_2^+ . This may be comparable to the $\cdot\text{CH}_2\text{OH}$ radical formed photochemically in the AgNa-A zeolite, the unpaired electron of which is attracted to the valence shell of silver to form an $\text{Ag}\cdot\text{CH}_2\text{OH}$ one-electron “half-bond” [22]. The possible interaction between the unpaired electron in AA' and the uranium center in UO_2^+ can prevent the electron from delocalizing to the ring, giving rise to a singlet EPR signal.

Similar to the UO_2^{2+} /alcohol and UO_2^{2+} / Ph_2S mixtures, the UV-Vis spectra of the initial mixtures of UO_2^{2+} (0.05 M, as the acetate salt) and L-ascorbic acid (AA) in the aqueous media containing H_2SO_4 (0.5 M) exhibited a strong absorption at 350–400 nm (Fig. 15b). This absorption became particularly strong when the AA concentration was greater than 0.4 M. The intensity of the absorption (represented by the absorbance A_{375} at 375 nm) was shown to be directly proportional to the molar concentrations of AA and UO_2^{2+} , respectively, showing formation of an EDA complex between UO_2^{2+} and AA in the initial reaction mixtures. The single-electron transfer process in Eq. (14) takes place within the EDA complex $[\text{UO}_2^{2+}, \text{AA}]$ as illustrated in Eq. (15).



3.5. Thermal charge-transfer reduction of uranyl UO_2^{2+} (VI) to UO_2^+ (V) by 2-methyl-5-(propan-2-yl)phenol (carvacrol)

2-Methyl-5-(propan-2-yl)phenol (carvacrol) is a biological antioxidant [23,24]. We carried out a thermal reduction of UO_2^{2+} (0.05 M, as the nitrate salt) by carvacrol at different concentrations (0.04 M, 0.09 M, and 0.22 M respectively) in acetone. The reaction mixtures were incubated in the dark at ambient temperature for 24 h and then characterized by EPR spectroscopy (Fig. 16). All the spectra in Fig. 16 exhibited a broad signal of UO_2^+ ($g = 2.06$) and a sharp singlet of 2-methyl-5-(propan-2-yl)phenoxyl (carvacrol radical, $g = 1.99$). The EPR results have shown that a single-electron transfer from the OH oxygen in carvacrol to the uranium valence shell in UO_2^{2+} took place to bring about the oxidation-reduction reaction (Eq. (16)).

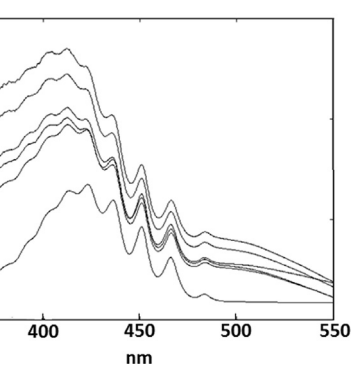
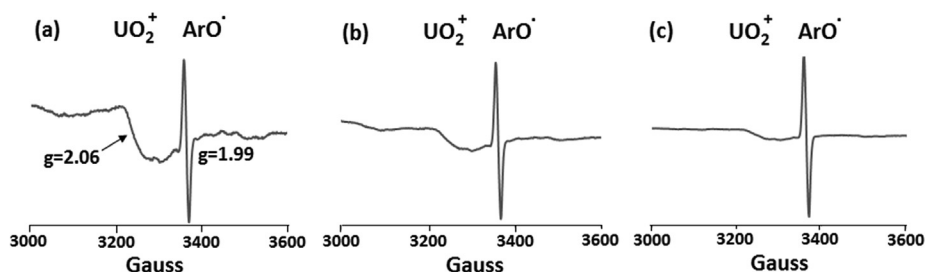


Fig. 17. The UV-Vis spectra of the initial mixtures of UO_2^{2+} (0.05 M, as the nitrate salt) and 2-methyl-5-(propan-2-yl)phenol (carvacrol, ArOH) at different concentrations in acetone. From bottom to top: $[\text{ArOH}] = 0.055$ M, 0.10 M, 0.27 M, 0.50 M, 0.76 M, 1.10 M. ($A_{375} = 0.809[\text{ArOH}] + 0.043$, $R^2 = 0.946$). The UV-Vis spectra of UO_2^{2+} (0–0.06 M) in the ArOH -acetone solutions (with $[\text{ArOH}] = 0.80$ M) were also recorded. ($A_{375} = 17.75[\text{UO}_2^{2+}] + 0.11$, $R^2 = 0.982$).

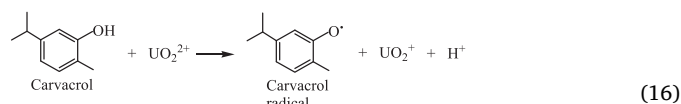
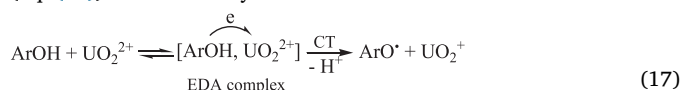


Fig. 16 also exhibited that the ratio of the intensity of carvacrol radical signal to intensity of the UO_2^+ signal increases as the initial concentration of carvacrol in the mixtures increases. The spin density (unpaired electron) in various phenoxyl radicals (ArO') has been demonstrated to undergo substantial delocalization to the aromatic ring [25]. In the presence of UO_2^+ , the unpaired electron in carvacrol radical can be possibly strongly attracted to the uranium valence shell of UO_2^+ , analogous to the above AA'/UO_2^+ interactions. This may have prevented the delocalization of the unpaired electron to the aromatic ring and gives rise to a sharp singlet EPR signal for carvacrol radical as seen in Fig. 16.

Analogous to the UO_2^{2+} /alcohol (methanol, ethanol, 2-propanol, and cyclohexanol) mixtures, UO_2^{2+} / Ph_2S mixtures, and UO_2^{2+} /ascorbic acid mixtures, the UV-Vis spectra of the initial mixtures of UO_2^{2+} (0.05 M, as the nitrate salt) and carvacrol (ArOH) in acetone exhibited a strong absorption at 350–400 nm (Fig. 17). The intensity of the absorption (represented by the absorbance A_{375} at 375 nm) has been shown to be directly proportional to the molar concentrations of ArOH and UO_2^{2+} , respectively, indicating the reversible formation of an EDA complex $[\text{ArOH}, \text{UO}_2^{2+}]$ between UO_2^{2+} and ArOH in the initial reaction mixtures. Comparable to the $[\text{UO}_2^{2+}, \text{Ph}_2\text{S}]$ complex, $[\text{ArOH}, \text{UO}_2^{2+}]$ is formed most likely via a weak oxygen \rightarrow uranium coordination bond. Then an irreversible single-electron transfer takes place within the EDA complex $[\text{ArOH}, \text{UO}_2^{2+}]$ to give ArO' and UO_2^+ (Eq. (17)) as observed by EPR.



It has been shown that the antioxidant activity of carvacrol is

Fig. 16. The EPR spectra of the mixtures of UO_2^{2+} (0.05 M, as the nitrate salt) and 2-methyl-5-(propan-2-yl)phenol (carvacrol, ArOH) at different concentrations in acetone recorded in the frozen state at 80 K after each mixture was incubated for 24 h in the dark at ambient temperature. (a) $[\text{ArOH}] = 0.04$ M, (b) $[\text{ArOH}] = 0.09$ M, and (c) $[\text{ArOH}] = 0.22$ M. All the spectra exhibit signals of UO_2^+ (broad, $g = 2.06$) and carvacrol radical ArO' (singlet, $g = 1.99$).

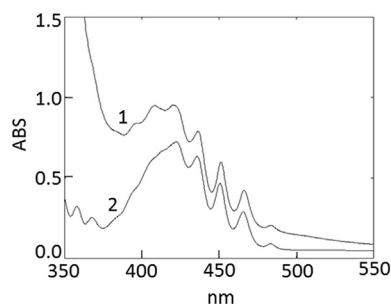
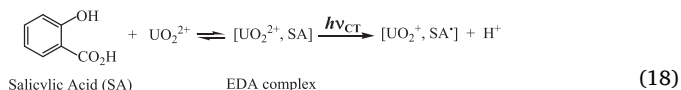


Fig. 18. Line 1 (top): The UV-Vis spectrum of an initial mixture of UO_2^{2+} (0.05 M, as the nitrate salt) and salicylic acid (0.75 M) in acetone, showing strong absorption at 375 nm; and Line 2 (bottom): The UV-Vis spectrum of an initial mixture of UO_2^{2+} (0.05 M, as the nitrate salt) and benzoic acid (0.75 M) in acetone, showing essentially no absorption at 375 nm.

directly related to the stability of the carvacrol radical [23,24]. The observation of the stable carvacrol radical in this work by EPR at ambient conditions has provided further supporting information for the studies of biological antioxidant functions of carvacrol.

Similar to carvacrol, salicylic acid (SA) also belongs to phenols (ArOH), but contains an electron withdrawing carboxyl ($-\text{CO}_2\text{H}$) group in the aromatic ring. The UV-Vis spectra of the UO_2^{2+} /SA mixtures exhibited analogous strong absorption at 350–400 nm (Fig. 18, Line 1). By comparison with a spectrum of UO_2^{2+} /benzoic acid (PhCO_2H) mixture which lacks the absorption at 375 nm (Fig. 18, Line 2), the absorption due to the carboxyl group in salicylic acid can be excluded. The absorption at 350–400 nm for salicylic acid is attributable to the charge-transfer transition from the hydroxyl ($-\text{OH}$) oxygen attaching to the aromatic ring to uranium in a $[\text{UO}_2^{2+}, \text{SA}]$ EDA complex reasonably formed via the interaction of the $-\text{OH}$ in the ring with the uranium center of UO_2^{2+} (Eq.18).



Due to the electron withdrawing $-\text{CO}_2\text{H}$, SA does not undergo thermal charge-transfer oxidation by UO_2^{2+} . After irradiated by Hg lamp (350 nm), a UO_2^{2+} -SA mixture in acetone exhibited weak EPR signals attributable to UO_2^+ and SA^\cdot (a phenoxy radical), supporting the photochemical charge-transfer redox between UO_2^{2+} and SA.

4. Conclusions

Thermal charge-transfer reductions of UO_2^{2+} (VI) by alcohols (methanol, ethanol, 2-propanol, and cyclohexanol), diphenyl sulfide (Ph_2S), ascorbic acid (AA), and 2-methyl-5-(propan-2-yl)phenol (carvacrol, ArOH) have been conducted. For each thermal reduction, both UO_2^+ (V) and a radical ($\cdot\text{CH}_2\text{OH}$, $\text{CH}_3\cdot\text{CHOH}$, $(\text{CH}_3)_2\text{COH}$, α -hydroxycyclohexyl, $\text{Ph}_2\text{S}^{\cdot+}$, AA^\cdot , or ArO^\cdot) have been identified by EPR spectroscopy, while only a radical, but not UO_2^+ (V), was observable in most of the photochemical reactions due to facile disproportionation of the initially formed UO_2^+ to UO_2^{2+} and U^{4+} in the light.

Spin-spin interactions between UO_2^+ and a radical ($\cdot\text{CH}_2\text{OH}$ or $\text{Ph}_2\text{S}^{\cdot+}$) have been evidenced from EPR studies. This and the UV-Vis studies together have supported the formations of the $[\text{UO}_2^+, \cdot\text{CH}_2\text{OH}]$

and $[\text{UO}_2^+, \text{Ph}_2\text{S}^{\cdot+}]$ ion-radical pairs in the course of the thermal redox reactions of UO_2^{2+} with CH_3OH and Ph_2S , respectively.

A ground-state charge-transfer mechanism has been developed for thermal reductions of UO_2^{2+} (VI) by methanol and diphenyl sulfide on the basis of EPR and UV-Vis studies (Eqs. (4) and (13)).

The sulfuric-acid-catalyzed isomerizations of $\cdot\text{CH}_2\text{OH}$ to $\text{CH}_3\text{O}^\cdot$ and $\text{CH}_3\cdot\text{CHOH}$ to $\text{CH}_3\text{CH}_2\text{O}^\cdot$ have been found by EPR studies. The identifications of the two alcohol radicals for methanol and ethanol have been confirmed by variable power EPR measurements.

Reduction of uranyl UO_2^{2+} (VI) to the lower oxidation states of uranium [such as U(V) and U(IV)] forms an interesting aspect of its chemistry. Among other things, it facilitates separation of uranium from aqueous media (the water system) [2]. The present research not only possesses academic significance, but may also have societal impacts in terms of radioactive waste (uranium) disposal.

Acknowledgement

This work was funded by a National Science Foundation (NSF) grant (Award # CHE1229498). It has also been supported financially by the University of Charleston through a faculty sabbatical leave (X.S.) and aided by the University Chemistry Program operating fund. We would like to thank Mr. Trevor Duncan, Mr. Roger Deal, and Ms. Joy Wu for helping obtain some UV-vis spectroscopic data.

References

- [1] J.J. Katz, G.T. Seaborg, L.R. Morss, *The Chemistry of the Actinide Elements*, Chapman and Hall, London, 1986, pp. 340–347.
- [2] X. Sun, D.R.J. Kolling, H. Mazagri, B. Karawan, C. Pierron, *Inorg. Chim. Acta* 435 (2015) 117–124.
- [3] M. Kumar, R.M. Kadam, A.R. Dhobale, M.D. Sastry, *J. Nucl. Radiochem. Sci.* 1 (2000) 77–80.
- [4] C. Miyake, T. Nakase, Y. Sano, *J. Nucl. Sci. Technol.* 30 (1993) 1256–1260.
- [5] M. Sarakha, M. Bolte, *J. Phys. Chem. A* 104 (2000) 3142–3149.
- [6] H.D. Burrows, *Inorg. Chem.* 29 (1990) 1549–1554.
- [7] M.E.D.G. Azenha, H.D. Burrows, S.J. Formosinho, M. de G.M. Miguel, *J. Chem. Soc. Faraday Trans. 1* (85) (1989) 2625–2634.
- [8] T.J. Kemp, M.A. Shand, *Inorg. Chem.* 25 (1986) 3840–3843.
- [9] S. Kannan, A.E. Vaughn, E.M. Weis, C.L. Barnes, P.B. Duval, *J. Am. Chem. Soc.* 128 (2006) 14024–14025.
- [10] S. Stoll, A. Schweiger, *J. Magn. Reson.* 178 (2006) 42–55.
- [11] S. Tsushima, *Inorg. Chem.* 48 (2009) 4856–4862.
- [12] J.A. Weil, J.R. Bolton, *Electron Paramagnetic Resonance: Elementary Theory and Practical Applications*, 2nd ed., John Wiley & Sons, Hoboken, New Jersey, 2007.
- [13] P.J. Sr Sullivan, W.S. Koski, *J. Am. Chem. Soc.* 85 (1963) 384–387.
- [14] R.J. Buszek, A. Sinha, J.S. Francisco, *J. Am. Chem. Soc.* 133 (2011) 2013–2015.
- [15] R.G. Denning, *J. Phys. Chem. A* 111 (2007) 4125–4143.
- [16] L.S. Natrajan, *Coordination Chem. Rev.* 256 (2012) 1583–1603.
- [17] A.A. Migdisov, H. Boukhalfa, A. Timofeev, W. Runde, R. Roback, A.E. Williams-Jones, *Geochimica et Cosmochimica Acta* 222 (2018) 130–145.
- [18] T. Harazono, S. Sato, H. Fukutomi, *Bull. Chem. Soc. Jpn.* 57 (1984) 768–770.
- [19] K.-X. Wang, J.-S. Chen, *Acc. Chem. Res.* 44 (2011) 531–540.
- [20] S.G. Thangavelu, C.L. Cahill, *Inorg. Chem.* 54 (2015) 4208–4221.
- [21] C.P. Baird, T.J. Kemp, *Prog. Reaction Kinetics* 22 (1997) 87–139.
- [22] J. Michalik, J. Sadlo, A. van der Pol, E. Reijerse, *Acta Chim. Scand.* 51 (1997) 330–333.
- [23] J. Mastelic, I. Jerkovic, I. Blazevic, M. Poljac-Blazi, S. Borovic, I. Ivancic-Bace, V. Smrecki, N. Zarkovic, K. Brcic-Kostic, D. Vikić-Topić, N. Müller, *J. Agric. Food Chem.* 56 (2008) 3989–3996.
- [24] N.V. Yanishlieva, E.M. Marinova, M.H. Gordon, V.G. Raneva, *Food Chemistry* 64 (1999) 59–66.
- [25] C. Xie, P.M. Lahti, C. George, *Org. Lett.* 2 (2000) 3417–3420.